

# Unveiling the singular dynamics in the cosmic large-scale structure

Cornelius Rampf,\* Uriel Frisch, and Oliver Hahn

*Laboratoire Lagrange, Université Côte d'Azur, Observatoire de la Côte d'Azur,  
CNRS, Blvd de l'Observatoire, CS 34229, 06304 Nice, France*

(Dated: February 2, 2022)

Gravitational collapse of cold dark matter leads to infinite-density caustics that seed the primordial dark-matter halos in the large-scale structure. The development of these caustics begins, generically, as an almost one-dimensional phenomenon with the formation of pancakes. Focusing on the one-dimensional case, we identify a landscape of so far unknown singularities in the particle acceleration that emerge after the first crossing of particle trajectories. We complement our fully analytical studies by high-resolution N-body simulations and find outstanding agreement, particularly shortly after the first crossing. We develop the methods in 1D but outline briefly the necessary steps for the 3D case.

*Introduction.*—Singularities are essential features in many disciplines, and their mathematical modelling sometimes comes with dramatic consequences. An important example are critical phenomena in phase transitions, which can be classified by their singularities (e.g., in the heat capacity); eventually, they have been successfully described by the renormalization group approach [1]. Singularities are also central in the field of optics [2, 3], where they prominently appear as caustics, giving rise, for example, to the ornate pattern of light on the seafloor as it passes through the waves on the surface.

In cosmology, caustic formation is the core process for making up the cosmic large-scale structure. At the particle level, infinite-density caustics result from shell-crossing, the crossing of cold dark matter (CDM) trajectories. Once particles have crossed for the first time, the single-stream flow enters into the multi-stream regime. Subsequently, secondary gravitational infall commences, inducing many more shell-crossings that lead to a proliferation of streams, and eventually to virialized structures.

Using an approximate nonlinear theory of gravitational instability, the Zel'dovich approximation (ZA; [4]), some of the singularities have been classified in the early 80s [5, 6]. However, singularities in the particle acceleration, which we report in the present Letter, remained undetected as the ZA is an acceleration-free model for the nonlinear collapse, thereby being effectively blind to the phenomenon of secondary gravitational infall.

Central to the analysis of [5, 6], as well as ours, is the use of Lagrangian-coordinates approaches to gravitational instability that allow to investigate singularities in a tractable manner. The ZA is the lowest-order Lagrangian-coordinates approximation to the cosmological fluid equations (the single-stream case of the Vlasov–Poisson equations), which furthermore becomes exact in 1D [7, 8], as long as multi-stream flow has not yet appeared. Beyond 1D, higher-order approximations should be incorporated, and the corresponding framework is dubbed Lagrangian perturbation theory (LPT) [9–15]. In LPT the particle trajectory, or like-

wise the displacement field, is the only dynamical variable, which is expanded perturbatively. Recently, the first nontrivial shell-crossing solutions in LPT have been identified [16, 17]. Even more recently, numerical evidence of convergence of LPT in 3D until shell-crossing was outlined in Ref. [18].

Nonetheless, even higher-order LPT is not able to predict secondary gravitational infall, due to the well-known breakdown of the cosmological fluid equations at the first shell-crossing. Instead the evolution of CDM is governed by the multi-stream Vlasov–Poisson equations. Following broadly in the footsteps of the initial studies [19–21], in this Letter we develop and exploit a theory for solving Vlasov–Poisson, thereby allowing us to detect so far unknown singularities. Details to the differences and further results are provided in a follow-up paper [22]. For the time being, we assume a Universe in 1D; the corresponding solutions play an important role in cosmology, mainly because 3D shell-crossings generically begin as almost 1D phenomena with the formation of pancakes [23, 24]. Notwithstanding, our theoretical tools are to a large extent scalable to any dimensions with only mild modifications. We shall come back to this in the conclusions.

*Setup.*—We restrict our analysis to an Einstein–de Sitter (EdS) cosmology, where the Universe is spatially flat and only filled with a CDM component. A cosmological constant and/or departing from spatial flatness can be easily incorporated if needed (cf. [25]). We denote by  $q \mapsto x(q, \tau)$  the Lagrangian map from initial ( $\tau=0$ ) position  $q$  to current position  $x$  at time  $\tau$ , where  $\tau$  is not the cosmic time  $t$  but is proportional to  $t^{2/3}$ . We make use of comoving coordinates  $x = r/a$ , where  $r$  is the proper space coordinate and  $a$  the cosmic scale factor (for an EdS universe  $a = \tau$ ). The velocity is expressed in terms of the convective time derivative of the map, i.e.,  $v(x(q, \tau), \tau) = \partial_\tau x(q, \tau) =: \dot{x}(q, \tau)$ . The Lagrangian evolution equation and the associated Poisson equation are respectively (see e.g. [26])

$$\ddot{x} + \frac{3}{2\tau} \dot{x} = -\frac{3}{2\tau} \nabla_x \varphi, \quad \nabla_x^2 \varphi = \frac{\delta}{\tau}, \quad (1)$$

where  $\delta := (\rho - \bar{\rho})/\bar{\rho}$  is the density contrast;  $\delta$  and  $\varphi$  explicitly depend on the map  $x(q, \tau)$ . Both theoretical and numerical N-body methods aim to solve those two equations, however with at least one substantial difference, namely that in N-body methods the density contrast is approximated by summing up N discrete particles over a fixed volume. By contrast, the theory of [20] uses a Green's function approach of nonlocal nature, while we determine the density, using the Dirac-delta " $\delta_D$ ", as

$$\delta(x(q, \tau), \tau) = \int \delta_D[x(q, \tau) - x(q', \tau)] dq' - 1, \quad (2)$$

which is amenable to local evaluations. The identity (2) is known (e.g. [27, 28]) however is used implicitly before shell-crossing, except in [21, 29].

Observe that Eqs.(1) are invariant under the non-Galilean coordinate transformation  $x \rightarrow x + \zeta_0(\tau)$ , where  $\zeta_0$  is an arbitrary function of time. This symmetry group has been first identified in [30], subsequently investigated in [12] and recently rediscovered in [31, 32] for deriving large-scale consistency relations. In the present context, we rather follow [12] and use the symmetry to *enforce the following center-of-mass condition* for the Lagrangian displacement field  $\xi(q, \tau) := x(q, \tau) - q$ ,

$$\int_{\mathbb{T}} \xi(q', \tau) dq' = 0, \quad \forall \tau > 0, \quad (3)$$

where  $\mathbb{T}$  stands for Torus. We emphasize that, in contrast to [12], we employ this physical condition also beyond the single-stream regime; it then becomes nontrivial with interesting consequences.

*Solution strategy and the initial conditions.*—Equations (1) can be easily combined into a single equation by first taking the Eulerian divergence of the former. Converting the remaining Eulerian derivatives according to  $\partial_x = (1/[\partial_q x])\partial_q$ , we first obtain

$$\partial_q \mathfrak{R}_\tau \xi = -\frac{3}{2} F(x(q, \tau)), \quad (4)$$

where  $\mathfrak{R}_\tau = \tau^2 \partial_\tau^2 + (3\tau/2)\partial_\tau - 3/2$ , and  $F(x(q, \tau)) := (\partial_q x) \int \delta_D[x(q, \tau) - x(q', \tau)] dq' - 1$  is the effective (multi-streaming) force. Integrating (4) in space from 0 to  $q$ , we then arrive at our evolution equation for the Lagrangian displacement field,

$$\mathfrak{R}_\tau \{\xi(q, \tau) - \xi_c(\tau)\} = -\frac{3}{2} S(x(q, \tau)). \quad (5)$$

Here,  $S(x(q, \tau)) := \int_0^q F(x(q', \tau)) dq'$  is the integrated multi-streaming force, and  $\xi_c(\tau) := \xi(q=0, \tau)$  is an integration constant which, as we show, *is generally nonzero in multi-streaming regions, by virtue of the center-of-mass-condition* (3). To solve (5), we provide growing-mode initial conditions [33], at  $\tau = 0$ ,

$$\xi(q, \tau=0) = -q + \frac{q^3}{6} + c q^4 + h.o.t. =: \xi_{ZA}^{(ini)}(q), \quad (6)$$

where  $c$  is a coefficient and *h.o.t.* denotes higher-order terms. Four remarks are in order. Firstly, we include a  $\sim q^4$  term, implying that in some sense we go one order higher than Refs.[19, 20]. Secondly, we assume that  $c$  is sufficiently small, which has the advantage that we can simplify some expressions by linearization. Thirdly, in principle, a higher-order term  $\sim q^6$  should be added in (6) to maintain the zero-average condition (3) in the single-stream regime. Lastly and most importantly, as we shall see, in the presence of a nonzero  $c$  in (6), a singular boost emerges at the first shell-crossing, as a consequence of maintaining the zero-average condition (3).

*Recovering the Zel'dovich solution.*—In the single-stream regime the integral in  $F$  simplifies as there is only a single root  $x(q, \tau) = x(q', \tau)$  that contributes to the integral, yielding an inverse  $\partial_q x$ ; thus  $F = 0$  and so is its integral,  $S = 0$ . Hence, Eq. (5) reduces to  $\mathfrak{R}_\tau \{\xi - \xi_c\} = 0$ . Furthermore, due to the absence of asymmetries in the evolution equation, we have, by virtue of the center-of-mass condition (3), that  $\xi_c = 0$ . Thus, the evolution equation can be solved with the initial condition (6), and we recover the well-known Zel'dovich solution [4, 7]

$$x_{ZA}(q, \tau) = q + \tau \xi_{ZA}^{(ini)}(q). \quad (7)$$

The Zel'dovich solution is only valid until the time of first shell-crossing, denoted with  $\tau_*$ , that is when the particle trajectory loses its single-valuedness and CDM enters into the multi-stream regime. For topological reasons (see Fig. 1), the first appearance of  $\partial_q x_{ZA} = 0$  marks this turning point, which, as is well known, is accompanied with an infinite density (cf. Eq. (2)):  $\delta(x_{ZA}(q, \tau_*)) = 1/[\partial_q x_{ZA}(q, \tau_*)] - 1 = \infty$ . It is easily checked that for the considered initial conditions, the first shell-crossing occurs at  $\tau_* = 1$  at  $q = 0$ , for sufficiently small  $c$ .

*Post-shell-crossing dynamics.*—To make progress on the analysis after shell-crossing, we introduce an iterative scheme for (5) in which the evolution of the post-Zel'dovich (PZA) displacement,  $\xi_{PZA}$ , is driven by an integrated force resulting from the Zel'dovich flow, i.e.,

$$\mathfrak{R}_\tau \{\xi_{PZA}(q, \tau) - \xi_c(\tau)\} = -\frac{3}{2} S_{ZA}(q, \tau) \quad (8)$$

in the first iteration, where explicitly  $S_{ZA}(q, \tau) := \int_0^q F(x_{ZA}(q', \tau)) dq'$ . Our iteration scheme is related to the one of [20] but there are differences; detailed comparisons and higher-order iterations will be presented in [22].

To determine  $\xi_{PZA}$ , we first need to solve for  $S_{ZA}$ , which amounts to finding the vanishing arguments of  $\delta_D[x_{ZA}(q, \tau) - x_{ZA}(q', \tau)]$ , and expressing the roots in terms of  $q$ . Shortly after shell-crossing, and given that  $c$  is small, there are three physical roots  $q_1, q_2$  and  $q_3$ , implying that  $F(x_{ZA}(q)) = [\partial_q x_{ZA}(q)]\{1/|\partial_q x(q_1)| + 1/|\partial_q x(q_2)| + 1/|\partial_q x(q_3)|\} - 1$ . For small positive  $c$ , the positions of the three roots are slightly shifted to the left,

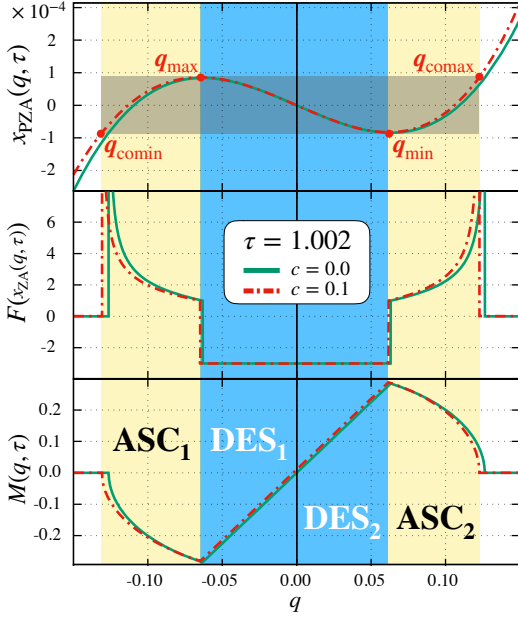


FIG. 1. Shown is the post-Zel'dovich map  $x_{\text{PZA}} = q + \xi_{\text{PZA}}$  (top panel), the corresponding multi-streaming force  $F$  (middle panel) as well as the source  $M$  (lower panel) of  $\Re_{\tau}\xi_{\text{PZA}}$ , which is a superposition of  $\Re_{\tau}\xi_c$  and the integrated force  $S = \int_0^q F(q')dq'$ . All plots are evaluated shortly after the first shell-crossing ( $\tau_{\star}=1$ ), namely at  $\tau=1.002$ . Green (solid) lines denote  $c=0$ , whereas red (dot-dashed) lines  $c=0.1$ . The grey (horizontally) shaded region marks the multi-streaming region (for  $c=0.1$ ), which spans up the ascending (**ASC**<sub>1</sub> and **ASC**<sub>2</sub>; yellow-shaded) and the descending (**DES**<sub>1</sub> and **DES**<sub>2</sub>; blue-shaded) multi-stream regimes. The single-stream regime has no shading. The sharp non-differentiable features in  $F$  and  $M$ , as well as the slight shift of  $F$  and  $M$  in the presence of nonzero  $c$ , are physical effects associated to singular behavior.

which can be calculated in perturbation theory, yielding

$$S_{\text{ZA}} = \begin{cases} 0; & 0 \leq \tau \leq \tau_{\text{com}} \\ -\text{sign}(q)\sqrt{D(q, \tau, c)}; & \tau_{\text{com}} \leq \tau \leq \tau_{\text{min}} \\ -3q; & \tau \geq \tau_{\text{min}} \end{cases} \quad (9)$$

to first order in  $c$ , where  $D = 24 - 3q^2 - 24/\tau + 24cq(3 - q^2 - 3/\tau)$ ,  $\tau_{\text{com}} = 8/(8 - q^2 - 5cq^3)$ , and  $\tau_{\text{min}} = 2/(2 - q^2 - 8cq^3)$ . Conversely, the Lagrangian positions can be expressed by  $\tau_{\text{com}}$  and  $\tau_{\text{min}}$ , leading to  $q_{\text{comin/comax}} = \mp\sqrt{8(1-1/\tau) - 20c(1-1/\tau)}$  and

$q_{\text{min/max}} = \pm\sqrt{2(1-1/\tau) - 8c(1-1/\tau)}$ , to first order in  $c$ . For convenience, we have marked those values by red dots in Fig. 1.

Before determining  $\xi_{\text{PZA}}$ , let us derive the integration constant  $\xi_c(\tau)$ . We apply the center-of-mass-condition (3) to the evolution equation (8), which amounts to integrating the latter in  $q$  from  $-\pi$  to  $\pi$ , i.e.,

$$\int_{-\pi}^{\pi} \Re_{\tau}\xi_{\text{PZA}}(q', \tau) dq' = \int_{-\pi}^{\pi} M(q', \tau) dq', \quad (10)$$

where  $M(q, \tau) := \Re_{\tau}\xi_c(\tau) - (3/2)S_{\text{ZA}}(q, \tau)$ . The l.h.s. of (10) must vanish by virtue of (3) and the fact that the integration commutes with the temporal operator, leaving us with  $0 = \int_{-\pi}^{\pi} M(q', \tau) dq'$ . We note that  $S_{\text{ZA}}$  (Eq. (9)) in  $M$  is only defined piecewise, rendering the averaging procedure nontrivial. We propose to tackle this by the Ansatz  $\xi_c = \xi_1 + \xi_2 + \xi_3$ , where the individual  $\xi_{1,2,3}$  are the solutions of the individual branches. For the single-stream regime we have from above  $\xi_1 = 0$ . For the other two we have  $\Re_{\tau}\xi_2 = -\langle (3/2)\text{sign}(q)\sqrt{D(q, \tau, c)} \rangle$ , and  $\Re_{\tau}\xi_3 = -\langle 9q/2 \rangle$ , where the brackets denote the spatial average weighted by the total length  $l$  of the spatial integration domain (e.g., for  $\xi_3$ ,  $l = q_{\text{min}} - q_{\text{max}}$ ). To first order in  $c$ , we find  $\Re_{\tau}\xi_2 = 18c(1 - 1/\tau)$ , and  $\Re_{\tau}\xi_3 = 36c(1 - 1/\tau)$ . Supplemented with the boundary conditions at shell-crossing  $\xi_2(\tau=1) = 0$ ,  $\dot{\xi}_2(\tau=1) = 0$ , and same for  $\xi_3$ , we obtain ( $\tau \geq \tau_{\text{min}}$ )

$$\xi_c(\tau) = -\frac{18c}{5} \left( 10 + 8\tau^{-3/2} - 15/\tau - 3\tau \right). \quad (11)$$

As we see,  $\xi_c$  is an effective time-dependent boost that switches on only after shell-crossing. The lower panel in Fig. 1 shows the combined effect of the boost  $\xi_c$  and the integrated multi-streaming force,  $M = \Re_{\tau}\xi_c - (3/2)S_{\text{ZA}}$ . After  $\tau_{\star}$ , the boost leads to the non-analytic movement of a particle that is initially at  $q = 0$  (right panel in Fig. 2), an effect that cannot be obtained from the ZA. Some indications of that boost, for random initial conditions, have been computed numerically in [21]; see their Fig. 5.

Having obtained the integrated force term and the boost, Eq. (8) can be solved by the method of variation of constants,  $\xi_{\text{PZA}} = \lambda(\tau)\tau + \mu(\tau)\tau^{-3/2}$ , with boundary conditions provided at shell-crossing, i.e.,  $\xi_{\text{PZA}}(\tau=1) = \xi_{\text{ZA}}^{(\text{ini})}$  and  $\dot{\xi}_{\text{PZA}}(\tau=1) = \dot{\xi}_{\text{ZA}}^{(\text{ini})}$ , where  $\xi_{\text{ZA}}^{(\text{ini})}$  is given in Eq. (6). Detailed calculations are presented in the follow-up paper [22], and lead to our main analytical result,

$$\xi_{\text{PZA}} = \xi_c(\tau) + \begin{cases} \tau\xi_{\text{ZA}}^{(\text{ini})}(q); & 0 \leq \tau \leq \tau_{\text{com}}; & \text{SIN} \\ \tau\xi_{\text{ZA}}^{(\text{ini})}(q) + \frac{\text{sign}(q)}{180} \frac{D^{5/2}(q, \tau, c)\tau}{8 - q^2 + cq(48 - 11q^2)}; & \tau_{\text{com}} \leq \tau \leq \tau_{\text{min}}; & \text{ASC} \\ -3q + \frac{4}{5}q\tau - \frac{17}{60}q^3\tau + \frac{48}{5} \sqrt{\frac{2}{2 - q^2}} \frac{q}{8 - q^2} \tau^{-3/2} + cf(q, \tau); & \tau \geq \tau_{\text{min}}; & \text{DES} \end{cases} \quad (12)$$

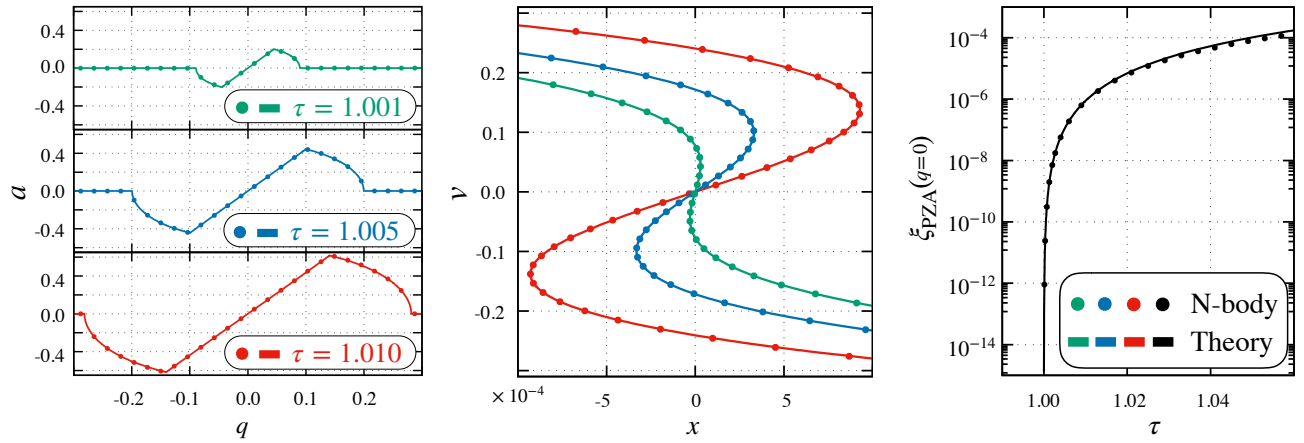


FIG. 2. Results of theory (solid lines) against high-resolution N-body simulations (dotted; only every 30th data point shown) after the first shell-crossing ( $\tau_* = 1$ ). The left panel shows the acceleration  $a := \ddot{x}_{\text{PZA}} = \ddot{\xi}_{\text{PZA}}$  as a function of the initial position  $q$  for  $c = 0$ , displaying four non-differentiable sharp features and thereby unveiling singular behavior (theory and numerics agree almost perfectly). The central panel shows the phase-space of our PZA result for  $c = 0$  at various times (as in first panel), which involves the typical phenomenon of multi-valuedness in position space due to shell-crossing. The right panel shows the sudden movement of a particle as a consequence of an asymmetry in the multi-streaming force starting at  $\tau_*$ , thereby marking non-analytic behavior and thus the emergence of another singularity (we set  $c = 0.1$ ).

where  $f(q, \tau) := \frac{11}{20}q^4\tau - \frac{36}{5}q^4\left(\frac{2}{2-q^2}\right)^{3/2}\frac{3q^2-4}{(q^2-8)^2}\tau^{-3/2}$ . In Fig. 1 we have shaded the ascending (**ASC**) and descending (**DES**) multi-stream branches, while the single-stream branch (**SIN**) has no shading.

*Asymptotics and singularities in space and time.*— Singularities in the PZA displacement (12) could originate from two distinct sources, either by (a) explicit non-analytic features within the piecewise defined branches of the map, and/or by (b) discontinuities that arise when “glueing” the branches together. Related to (a), it is easily checked that the only non-analyticity within the branches arise when the discriminant  $D$  vanishes, which occurs at  $\tau_{\text{com}}$ . Related to (b), two other singularities are revealed at  $\tau_{\text{min}}$ .

To identify the (a)-type singularity it suffices to limit ourselves to  $c = 0$ . Indeed, a vanishing discriminant  $D$  is achieved by freezing the space dependence in  $D$  and investigating small discrepancies  $\delta\tau > 0$  around  $\tau_{\text{com}}$  from above. Taylor-expanding the term with the discriminant around  $\delta\tau$  then leads to the identification of a  $\delta\tau^{5/2}$  singularity. Similarly, by freezing the time and varying  $q$ , one finds spatial singularities at  $q_{\text{comax/comin}}$  with exponent  $5/2$ . Physically, what happens is that a spectator particle near  $q_{\text{comax/comin}}$  crosses a caustic at the current (Eulerian) position.

The (b)-type singularities are expected to occur at  $\tau_{\text{min}}$ . One of those singularities stems from glueing the ascending and descending multi-stream branches together, for which purpose it suffices to set  $c = 0$ . Taylor-expanding around small temporal discrepancies near  $\tau_{\text{min}}$ , we find that the third-order time derivative

flips sign, indicating that the third derivative of  $\xi$  is discontinuous, thereby marking a singularity of  $\xi \sim (\tau - \tau_{\text{min}})^3 \theta(\tau_{\text{min}} - \tau)$ . Similarly, we find that also the third spatial derivative of the map is discontinuous, thus implying spatial singularities near  $q_{\text{min/max}}$  of exponent 3.

Lastly, a nontrivial singularity originates from  $\xi_c$  (Eq. (11)), which is driven by a forcing asymmetry (from  $c \neq 0$  in the initial conditions); this manifests itself through *the loss of analyticity at the first shell-crossing, thereby resulting in a nontrivial phase transition*. Indeed, the boost  $\xi_c$  “switches” from off to on ( $\propto \delta\tau^3$ ), once multi-streaming develops (see right panel in Fig. 2). Consequently, a particle that is initially at  $q = 0$  will remain there until  $\tau_*$ , but then the first time-derivative of its acceleration receives a non-analytic kick, jumping from 0 to a finite number.

The (a)-type and first (b)-type singularities are shown in the first panel of Fig. 2 ( $c = 0$ ), while the second (b)-type singularity is displayed in the third panel, for  $c = 0.1$ . We confront these findings against high-precision numerical simulations; the results are marked by dots in Fig. 2. The respective code, which we make publicly available,<sup>1</sup> is a one-dimensional, symplectic time-integrating scheme that determines the force by an efficient particle sorting algorithm. Periodic initial conditions with vanishing mean are provided by the ZA. Most runs were performed with around  $10^4$  time-steps and particles, though for detecting the singularity stemming from  $\xi_c$ , temporal and spatial resolutions of up to  $10^5$  have been used.

<sup>1</sup> [https://bitbucket.org/ohahn/cosmo\\_sim\\_1d](https://bitbucket.org/ohahn/cosmo_sim_1d)

*Conclusions.*—Cold dark matter is assumed to have zero temperature, which, as we have shown, leads to non-differentiable acceleration features after shell-crossing (derivatives blow up!). We have provided a novel theory to identify the nature of the singularities. Two of those singularities are of local origin and appear either when a particle enters a multi-streaming region, or when a particle swaps sides in the ascending (**ASC**) and descending (**DES**) multi-stream regimes (see Fig. 1, and first panel in Fig. 2). A third singularity is of *global origin* coming naturally from fixing a usually ignored integration constant  $\xi_c(\tau)$  in the evolution equations; *namely by considering spatial averages of Vlasov–Poisson*.

Most interestingly, the integration constant  $\xi_c(\tau)$  (cf. Eq. (11)) amounts to a non-Galilean boost that *affects all particles within the descending multi-stream regime*, but not others. Thus,  $\xi_c(\tau)$  is crucial for multi-streaming, except in exactly symmetric cases ( $c=0$ ), which are however perfectly degenerate and have zero probability to occur in a Universe with random initial conditions.

The most straightforward, yet challenging extension to our work is to exploit the singularity theory for Vlasov–Poisson in quasi-1D, where departures from 1D are perturbatively small, thus providing a bookkeeping parameter (cf. [16]). Generalizations to 3D are feasible as well, by using higher-order LPT [15, 25, 34] and providing boundary conditions at shell-crossing, especially for trigonometric initial conditions, where fast Fourier transforms can be avoided (cf. [18]). In this work, we have provided the stepping stones for such avenues; indeed, the central equations (1)–(3) are trivially generalized to arbitrary dimensions.

A full-fledged theory for Vlasov–Poisson has the potential to advance theoretical predictions for the large-scale structure, thereby, ultimately, allowing us to better interpret survey data. For example, the theory can provide *theoretical inputs* for heavily used effective theories of the large-scale structure [35–38]. Indeed, such effective theories incorporate shell-crossing and multi-streaming effects through counter terms (with *a priori* unknown time dependence), which are usually estimated from N-body simulations.

Lastly, Vlasov–Poisson equations are extensively used also beyond the realm of cosmology, for example in plasma physics, where, in the longrun, theoretical inputs could provide precious information for its mathematical analysis.

*Acknowledgements.*—We thank Zachary Slepian and Matias Zaldarriaga for useful discussions. CR acknowledges funding from the People Programme (Marie Skłodowska–Curie Actions) of the European Union H2020 Programme under Grant Agreement No. 795707 (COSMO-BLOW-UP). UF acknowledges financial support from the Université de la Côte d’Azur under Grant Agreement No. ANR-15-IDEX-01 (2018-2019). OH acknowledges funding from the European Research Coun-

cil (ERC) under the European Union’s Horizon 2020 research and innovation programme (Grant Agreement No. 679145, project ‘COSMO-SIMS’).

- 
- \* cornelius.rampf@oca.eu; Marie Skłodowska–Curie Fellow
- [1] K. G. Wilson and M. E. Fisher, Phys. Rev. Lett. **28**, 240 (1972).
  - [2] M. V. Berry, Journal of Physics A: Mathematical and General **10**, 2061 (1977).
  - [3] M. V. Berry and C. Upstill, Progress in Optics **18**, 257 (1980).
  - [4] Ya. B. Zel’dovich, A&A **5**, 84 (1970).
  - [5] V. I. Arnol’d, *Mathematical Methods of Classical Mechanics* (Springer, New York, 1980).
  - [6] V. I. Arnold, S. F. Shandarin, and Ya. B. Zeldovich, Geophys. Astrophys. Fluid Dyn. **20**, 111 (1982).
  - [7] E. A. Novikov, Sov. Phys. JETP **30**, 512 (1970), [Zh. Eksp. Teor. Fiz. 57, 938 (1969)], arXiv:1001.3709 [physics.gen-ph].
  - [8] A. S. Zentsova and A. D. Chernin, Astrophysics **16**, 108 (1980).
  - [9] T. Buchert and G. Goetz, J. Math. Phys. **28**, 2714 (1987).
  - [10] F. R. Bouchet, R. Juszkiewicz, S. Colombi, and R. Pellat, ApJ **394**, L5 (1992).
  - [11] T. Buchert, MNRAS **254**, 729 (1992).
  - [12] J. Ehlers and T. Buchert, Gen. Relativ. Grav. **29**, 733 (1997).
  - [13] F. Bernardeau, S. Colombi, E. Gaztanaga, and R. Scoccimarro, Phys. Rep. **367**, 1 (2002), arXiv:astro-ph/0112551 [astro-ph].
  - [14] C. Rampf and T. Buchert, JCAP **1206**, 021 (2012), arXiv:1203.4260 [astro-ph.CO].
  - [15] V. Zheligovsky and U. Frisch, J. Fluid Mech. **749**, 404 (2014), arXiv:1312.6320 [math.AP].
  - [16] C. Rampf and U. Frisch, MNRAS **471**, 671 (2017), arXiv:1705.08456 [astro-ph.CO].
  - [17] C. Rampf, MNRAS **484**, 5223 (2019), arXiv:1712.01878 [astro-ph.CO].
  - [18] S. Saga, A. Taruya, and S. Colombi, Phys. Rev. Lett. **121**, 241302 (2018), arXiv:1805.08787 [astro-ph.CO].
  - [19] S. Colombi, MNRAS **446**, 2902 (2015), arXiv:1411.4165 [astro-ph.CO].
  - [20] A. Taruya and S. Colombi, MNRAS **470**, 4858 (2017), arXiv:1701.09088 [astro-ph.CO].
  - [21] M. Pietroni, JCAP **1806**, 028 (2018), arXiv:1804.09140 [astro-ph.CO].
  - [22] U. Frisch and C. Rampf, in preparation (2019).
  - [23] A. L. Melott and S. F. Shandarin, ApJ **343**, 26 (1989).
  - [24] A. L. Melott and S. F. Shandarin, ApJ **410**, 469 (1993).
  - [25] C. Rampf, B. Villone, and U. Frisch, MNRAS **452**, 1421 (2015), arXiv:1504.00032 [astro-ph.CO].
  - [26] C. Uhlemann, C. Rampf, M. Gosenca, and O. Hahn, Phys. Rev. **D99**, 083524 (2019), arXiv:1812.05633 [astro-ph.CO].
  - [27] A. N. Taylor and A. J. S. Hamilton, MNRAS **282**, 767 (1996), arXiv:astro-ph/9604020 [astro-ph].
  - [28] T. Matsubara, Phys. Rev. **D77**, 063530 (2008), arXiv:0711.2521 [astro-ph].
  - [29] P. McDonald and Z. Vlah, Phys. Rev. **D97**, 023508 (2018), arXiv:1709.02834 [astro-ph.CO].

- [30] O. Heckmann and E. Schücking, *Zeitschrift für Astrophysik* **38** (1955), [in German].
- [31] A. Kehagias and A. Riotto, *Nucl. Phys.* **B873**, 514 (2013), arXiv:1302.0130 [astro-ph.CO].
- [32] M. Peloso and M. Pietroni, *JCAP* **1305**, 031 (2013), arXiv:1302.0223 [astro-ph.CO].
- [33] Y. Brenier, U. Frisch, M. Henon, G. Loeper, S. Matarrese, R. Mohayaee, and A. Sobolevskii, *MNRAS* **346**, 501 (2003), arXiv:astro-ph/0304214 [astro-ph].
- [34] T. Matsubara, *Phys. Rev.* **D92**, 023534 (2015), arXiv:1505.01481 [astro-ph.CO].
- [35] D. Baumann, A. Nicolis, L. Senatore, and M. Zaldarriaga, *JCAP* **1207**, 051 (2012), arXiv:1004.2488 [astro-ph.CO].
- [36] J. J. M. Carrasco, M. P. Hertzberg, and L. Senatore, *JHEP* **09**, 082 (2012), arXiv:1206.2926 [astro-ph.CO].
- [37] R. A. Porto, L. Senatore, and M. Zaldarriaga, *JCAP* **1405**, 022 (2014), arXiv:1311.2168 [astro-ph.CO].
- [38] T. Baldauf, L. Mercolli, M. Mirbabayi, and E. Pajer, *JCAP* **1505**, 007 (2015), arXiv:1406.4135 [astro-ph.CO].